

# Hybrid Geographic Routing for Flexible Energy–Delay Tradeoff

Min Chen, *Member, IEEE*, Victor C. M. Leung, *Fellow, IEEE*, Shiwen Mao, *Senior Member, IEEE*, Yang Xiao, *Senior Member, IEEE*, and Imrich Chlamtac, *Fellow, IEEE*

**Abstract**—Several geographic (or position-based) routing protocols have been proposed for data dissemination in wireless sensor networks. In these protocols, routing is based on the positions of neighboring nodes. In particular, the next-hop node is selected according to either a distance-based strategy, which favors a neighbor with the largest distance progress toward the sink, or a direction-based strategy, which favors a neighbor with the lowest angle deviation toward the sink. In this paper, we propose a novel hybrid geographic routing (HGR) scheme that combines both distance- and direction-based strategies in a flexible manner. To further facilitate a tradeoff between energy consumption and end-to-end delay, we propose two dynamic HGR (DHGR) mechanisms based on the basic HGR scheme, which are designed to satisfy constraints on the average end-to-end delay of specific applications while minimizing energy consumption. Packet-delivery decisions are locally made, and the state at a node is independent of the number of nodes in the network; thus, DHGR has the inherent scaling property of geographic routing. The effectiveness of the proposed schemes is evaluated by analysis and extensive simulations.

**Index Terms**—Energy efficiency, geographic routing, quality of service (QoS), wireless sensor networks (WSNs).

## I. INTRODUCTION

**I**N RECENT YEARS, we have witnessed a growing interest in deploying microsensors that collaborate in a distributed manner on data gathering and processing [1]. Due to limited resources at sensor nodes, routing in wireless sensor networks

(WSNs) is a challenging task [2]. Minimizing energy consumption has been considered an important problem and has been addressed with various approaches, e.g., the construction of special broadcast trees [3] and the combination of sleep/awake and probabilistic forwarding techniques [4]. A number of topology-based routing protocols (e.g., directed diffusion [5]) have been proposed, which establish routes on demand. However, these protocols typically require flooding of control packets over the network, which is costly in terms of power consumption and bandwidth requirement. In contrast, geographic routing protocols are inherently robust to topology changes (e.g., due to energy depletion or malfunction), because they can simply select another neighbor as the next hop if the previously selected neighbor is no longer available. In geographic routing protocols, packet forwarding decision is locally made based on node locations (i.e., those of the sink node, the current node, and its neighbors). No networkwide structuring or data exchange is needed, potentially achieving energy efficiency.

There are two basic greedy forwarding strategies in geographic routing: 1) the distance-based strategy and 2) the direction-based strategy. In the distance-based strategy, a routing protocol selects the neighbor node that is closest to the sink as the next hop [6]–[8], whereas in the direction-based strategy, a routing protocol selects a neighbor node whose deviation angle from the line that connects the current node and the sink is the minimum among all neighbors [9]. In this paper, we propose a novel routing scheme called hybrid geographic routing (HGR), which combines these two selection criteria to select a node with a large distance progress but a small deviation angle. To weigh the impact of distance- and direction-based criteria, an adjustment factor (denoted by  $\alpha$ ) is introduced. Extensive simulations show that HGR achieves a flexible tradeoff between energy consumption and end-to-end delivery latency. This tradeoff is enabled by using different values for the adjustment factor, which allows HGR to achieve superior performance with regard to energy consumption and end-to-end packet delivery latency over conventional distance- and direction-based algorithms if used separately.

Considering that the sensory data of different applications have different deadlines, we seek to adjust  $\alpha$  to satisfy end-to-end delay constraints while minimizing energy consumption. We propose two methods of  $\alpha$  adjustment to enhance HGR [called dynamic HGR (DHGR)] to ensure that localized forwarding decisions in HGR can globally achieve end-to-end quality-of-service (QoS) objectives, particularly in terms of

Manuscript received June 26, 2008. First published June 19, 2009; current version published November 11, 2009. This work was supported in part by the Canadian Natural Sciences and Engineering Research Council under Grant STPGP 322208-05 and in part by the IT R&D program of MKE/IITA [2007-F-038-03, Fundamental Technologies for the Future Internet] under Grant IITA-2009-C1090-0902-0006. The work of S. Mao was supported in part by the U.S. National Science Foundation (NSF) under Grant ECCS-0802113 and through the Wireless Internet Center for Advanced Technology, Auburn University, Auburn, AL. The work of Y. Xiao was supported in part by the NSF under Grant CCF-0829827, Grant CNS-0716211, and Grant CNS-0737325. Any opinions, findings, and conclusions or recommendations expressed in this paper are those of the authors and do not necessarily reflect the views of the NSF. The review of this paper was coordinated by Prof. A. Boukerche.

M. Chen is with the School of Computer Science and Engineering, Seoul National University, Seoul 151-744, Korea (e-mail: mchen@mmlab.snu.ac.kr).

V. C. M. Leung is with the Department of Electrical and Computer Engineering, University of British Columbia, Vancouver, BC V6T 1Z4, Canada (e-mail: vleung@ece.ubc.ca).

S. Mao is with the Department of Electrical and Computer Engineering, Auburn University, Auburn, AL 36849-5201 USA (e-mail: smao@ieee.org).

Y. Xiao is with the Department of Computer Science, University of Alabama, Tuscaloosa, AL 35487 USA (e-mail: yangxiao@ieee.org).

I. Chlamtac is with Create-Net, 38100 Trento, Italy, and also with the University of Trento, 38122 Trento, Italy (e-mail: chlamtac@create-net.org).

Color versions of one or more of the figures in this paper are available online at <http://ieeexplore.ieee.org>.

Digital Object Identifier 10.1109/TVT.2009.2025767



based approach, direction-based schemes intend to obtain a path with a shorter end-to-end Euclidean distance; however, more hop counts are likely to be needed [24].

In a seminal work [10], the proposed distance-routing-effect algorithm for mobility (DREAM) considers both direction and distance effects. It aims at minimizing the total number of control packets in the network with node mobility based on the fact that the farther the destination and the slower the rate of movement of the updating node, the less the frequency that a copy of the control packet needs to be sent. In contrast, this paper addresses the problem of meeting real-time constraints, which is often necessary for communications in real-world applications. In surveillance systems, for example, communication delays within the loops of sensing and actuating directly affect the quality of tracking.

There are a few studies that address time-sensitive traffic transmissions over WSNs. Chen *et al.* proposed directional geographical routing [15] to explore the application-specific number of node-disjoint routing paths to enlarge the aggregate bandwidth for the QoS provisioning in wireless multimedia sensor networks (WMSNs). The authors further presented a multiple-priorities-based path-scheduling algorithm [16] to guarantee the end-to-end transmission delay while balancing energy and bandwidth usage among all the node-disjoint paths in WMSNs. Shu *et al.* proposed two-phase geographic greedy forwarding [17] for geographic forwarding by taking into account both the requirements of real-time multimedia transmission and the realistic characteristics of WMSNs. Yuan *et al.* [18] proposed an integrated energy-and-QoS-aware transmission scheme for WSNs, in which the QoS requirements in the application layer and the modulation and transmission mechanisms in the link and physical layers are jointly optimized.

For service differentiation in the timeliness domain, energy-efficient differentiated directed diffusion (EDDD) [19] provides differentiated services for real-time and best effort traffic. However, it cannot scale well to WSNs of large size due to the requirement of global topology information. This shortcoming can be addressed by geographic routing approaches. SPEED [11] is a geographic routing scheme that was designed to provide soft end-to-end deadline guarantees for real-time packets in WSNs. Each node maintains neighbor node information, e.g., geographic distance and average delay, to each neighbor. Using the distance and delay, each node evaluates the packet progress speed of each neighbor node and forwards a packet to a node whose progress speed is higher than the prespecified lower bound speed. The multipath and multi-SPEED routing protocol [12] extends SPEED to support QoS provisioning in the timeliness and reliability domains.

### III. BASIC HYBRID GEOGRAPHIC ROUTING

In this section, we first review the distance- and direction-based criteria. In Section III-B, we then consider both distance and direction in the routing process. By adjusting the weights of distance and direction in the next-hop selection criteria, a wide array of application-specific delay requirements can be satisfied while achieving energy conservation.

TABLE II  
PSEUDOCODE FOR THE JOINT DISTANCE- AND DIRECTION-BASED ROUTING DECISION AT NODE  $h$

01	<b>procedure</b> NextHopSelection( $V_h$ )
02	<b>begin</b>
03	$V_h$ is the set of node $h$ 's neighbors in the forwarding area;
04	<b>for</b> each neighbor $i$ in $V_h$
05	Compute $\theta_i$ (or $y_i$ ), $x_i$ , as illustrated in Section III-A;
06	Compute $Q_i$ based on the joint distance- and direction-based criterion;
07	<b>endfor</b>
08	Select node $k$ as NextHop, where $k = \operatorname{argmax}\{Q_i   i \in V_h\}$ ;

The idea of energy–delay tradeoff is motivated by an interesting feature of some sensor devices, which can be exploited to reduce energy consumption [20]. That is, the sensor node has the capability to transmit at different power levels [21]. Assuming free space transmissions with a path loss exponent of 2 [22], the per-hop energy is proportional to the square of the hop distance.<sup>1</sup> The distance-based scheme intends to maximize progress; thus, it may introduce a larger hop distance than the direction-based scheme. From the viewpoint of statistics, the distance-based scheme intends to consume higher energy along the path toward the sink node, whereas the direction-based scheme yields smaller path energy consumption but results in larger hop counts with higher end-to-end delay [24].

#### A. Distance- and Direction-Based Criteria

As illustrated in Fig. 1, let  $x_i$  denote the projected progress of node  $i$ . Let  $\theta_i$  denote the deviation angle between the line that connects  $h$  with  $i$  and the line that connects  $h$  with  $t$ . When node  $i$  receives a data packet from  $h$ , the positions of its upstream node  $h$  ( $x_h, y_h$ ) and the sink  $t$  ( $x_t, y_t$ ) are piggybacked in the packet. Node  $i$  can next calculate the deviation angle by  $\theta_i = \arccos((D_h^i)^2 + (D_h^t)^2 - (D_i^t)^2 / 2D_h^i \cdot D_h^t)$ , where  $D_h^i$  is the distance between nodes  $h$  and  $i$ ,  $D_h^t$  is the distance between nodes  $h$  and  $t$ , and  $D_i^t$  is the distance between nodes  $i$  and  $t$ . The projected progress can then be calculated as  $x_i = D_h^i \cdot \cos(\theta_i)$ .

In this paper,  $x_i$  is considered as the distance-based criterion for node  $i$ , whereas  $\theta_i$  or  $y_i = D_h^i \cdot \sin(\theta_i)$  is considered to be the direction-based criterion for node  $i$ .<sup>2</sup>

#### B. Joint Distance- and Direction-Based Routing Decision

Let  $Q_i$  indicate node  $i$ 's eligibility (or priority) as the next hop. The greater  $x_i$  is, the larger  $Q_i$  becomes, whereas the lower  $\theta_i$  is, the larger  $Q_i$  becomes. We can define different forms for  $Q_i$  to combine both the distance- and direction-based routing criteria. For example,  $Q_i$  can be evaluated by  $Q_i = (1 - (|\theta_i|/90^\circ))^2 + (x_i/R)^2$ , where  $R$  denotes the transmission range. As another example, the joint distance- and direction-based routing criterion can be defined as  $Q_i = (1 - (y_i/R))^2 + (x_i/R)^2$ .

Table II shows the pseudocode of the joint distance- and direction-based next-hop selection algorithm, which selects the neighbor with the maximum  $Q_i$  as the next-hop node.

<sup>1</sup> Other propagation models, e.g., the two-ray ground model [22] and models with different path loss exponents, will give a different expression for the energy consumption, but the same trend will be observed.

<sup>2</sup>  $y_i$  is the distance between node  $i$  and its projected Point 1 in Fig. 1.

### C. Weighted Joint Routing Decision

The  $Q_i$  definitions in Section III-B are deterministic in the sense that the relative weights of distance- and direction-based criteria are fixed. To adjust the impact of  $x_i$  on node  $i$ 's eligibility as the next-hop node, we can incorporate a weight factor (with exponent  $\alpha$ ) into the basic criteria in Section III-B. Two examples of the weighted criteria are shown in (1) and (2) (there can also be some other variations; however, all the weighted hybrid criteria should follow a common law, i.e., when  $\alpha$  is small, its second term is negligible, and the routing mechanism operates like a direction-based scheme, whereas when  $\alpha$  is large, the second term in the equation dominates the first term, and the routing mechanism operates like a distance-based scheme):

$$Q_i = \left(1 - \frac{|\theta_i|}{90^\circ}\right)^2 + 2^\alpha \cdot \left(\frac{x_i}{R}\right)^2, \quad \alpha \in \mathcal{Z} \quad (1)$$

$$Q_i = (1 - \alpha) \cdot \left(1 - \frac{|\theta_i|}{90^\circ}\right)^2 + \alpha \cdot \left(\frac{x_i}{R}\right)^2, \quad \alpha \in [0, 1]. \quad (2)$$

### D. Flexible Energy–Delay Tradeoff

We have experimented with numerous definitions of weighted criteria. Among the variants, the criterion in (1) shows the most distinct tradeoff between distance and direction, which facilitates parameter tuning, as shown in Fig. 2. Thus, we define the weighted criterion in (1) as our basic HGR criterion in the remaining part of this paper. The HGR strategy is proposed to enhance the energy efficiency of scalable transmission for delay-sensitive traffic by performing tradeoffs between energy and delay, depending on the network dynamics and application requirements in WSNs.

To verify the impact of  $\alpha$  on HGR in terms of energy and delay, we vary  $\alpha$  from  $-7$  to  $7$  in (1) and carry out extensive simulation studies. As shown in Fig. 2, the energy and delay of both direction- and distance-based schemes remain constant, because changing  $\alpha$  has no effect on them. In comparison, it can be observed that energy and delay exhibit a tradeoff relation with regard to  $\alpha$  in HGR. As expected, for negative values of  $\alpha$ , HGR behaves like a direction-based scheme, which achieves lower energy consumption, whereas for positive values of  $\alpha$ , HGR behaves like a distance-based scheme, which yields lower delay. Fig. 2 clearly illustrates the energy–delay tradeoffs in HGR, where a higher  $\alpha$  value results in lower delay but, simultaneously, higher energy consumption due to the larger hop distance. Given a certain delay requirement, it is desirable to adjust  $\alpha$  to a value as low as possible to minimize energy consumption while satisfying the delay requirement.

### E. Dead-End Problem During Next-Hop Selection in HGR

The so-called dead-end problem arises when a packet is forwarded to a local minimum [25], [26]. If the current node does not have any neighbor that is closer to the sink, HGR will be performed in the recovery mode, where the downstream node is selected according to the face routing criterion to

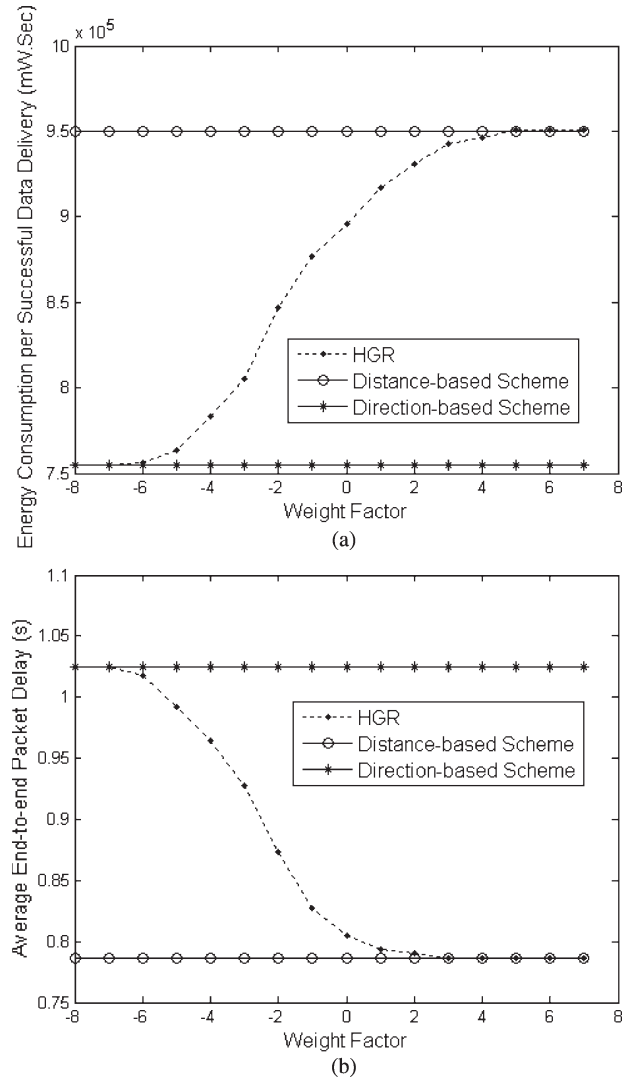


Fig. 2. Energy–delay tradeoffs in HGR. (a) Impact of  $\alpha$  on energy. (b) Impact of  $\alpha$  on delay.

recover from the local minimum [6]–[8]. To avoid loops and traverse mazes in the recovery mode, the downstream node is selected on the faces of a locally extracted planar subgraph, i.e., the Gabriel graph. When an intermediate node that receives a data packet is closer to the sink than the node where next-hop selection entered the recovery mode, the next-hop-selection algorithm switches back to the normal HGR selection mode, as described earlier in this section. The additional delay, which is introduced in the recovery mode, will be compensated in the following hops where the  $\alpha$  value is adjusted.

### F. Handling Link/Node Failures

In unreliable communication environments, traditional geographic routing protocols may fail to deliver data in a timely manner. Two fault-tolerant low-latency algorithms that meet sensor network requirements are proposed in [27]. A cluster-based structure is considered, which is different from this paper. When a link/node failure happens, the medium access control (MAC) layer cannot deliver the packet to an unreachable next-hop node. After several retransmission attempts, the MAC layer

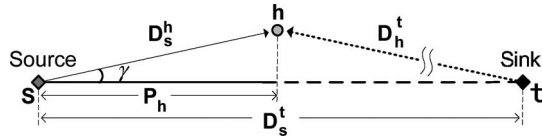


Fig. 3. Calculating the projected progress.

either just drops the packet or notifies the routing protocol of the failed transmission. The routing protocol, in turn, selects a different backup next hop and again hands the packet down to the MAC layer. This process is repeated until the packet is eventually delivered to the next hop. Thus, energy could be wasted on retransmissions, and the failover latency could be increased.

When a packet is lost due to channel failure, a receiver-oriented approach can be used to avoid acknowledgment transmission [28]. In the case that node  $i$  fails in data reception, rather than letting the upstream node retransmit the packet, another neighbor (e.g., node  $j$  in Fig. 1) that is suboptimal according to HGR but overhears the previous transmission can further forward the packet toward the sink.

#### IV. DYNAMIC HYBRID GEOGRAPHIC ROUTING

In the basic HGR, the  $\alpha$  value is fixed for data delivery between every source–destination pair. Unless we know the exact relation of  $\alpha$  to the delay *a priori*, it is unlikely that the source can select an optimal  $\alpha$  to minimize the energy consumption while satisfying the application’s delay requirement due to the network dynamics in WSNs.

In addition, although we can adopt sink–source feedback for adjusting  $\alpha$  to satisfy the required end-to-end delay constraint, the feedback information may become stale when it is received by a source node after some delay, particularly in the case with large hop counts between the source node and the sink. Thus, we seek distributed methods to adjust  $\alpha$  at each intermediate node during data dissemination based on local information, e.g., the position of the node, the location of the upstream (previous-hop) node, and the locations of the source and sink piggybacked in data packets.

In this section, we define DHGR as HGR with dynamic  $\alpha$  adjustment. We first present the problem statement for DHGR. We then propose two methods that allow each intermediate node to distributedly adjust  $\alpha$  without exchanging additional control messages along a path between the sink and source to satisfy application-specific end-to-end delay requirements.

##### A. Problem Statement

Let  $D_s^h$  be the distance from the source to node  $h$ ,  $D_h^t$  be the distance from  $h$  to the sink, and  $D_s^t$  be the distance from the source to the sink. The angle  $\gamma$  in Fig. 3 is equal to  $\arccos((D_s^h)^2 + (D_s^t)^2 - (D_h^t)^2 / 2D_s^h \cdot D_s^t)$ . Let  $P_h$  be the projected progress from the source to the current node  $h$ . It follows that

$$P_h = D_s^h \cdot \cos(\gamma). \tag{3}$$

Let  $T_{QoS}$  denote the application-specific delay requirement (i.e., the maximum delay allowed). Let  $t_s^h$  be the actual delay

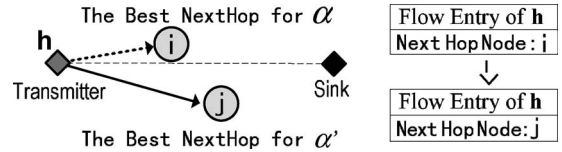


Fig. 4. Updating the next hop in the reference-value-based  $\alpha$  adjustment.

of the data packet from source  $s$  to the current node  $h$ . Then,  $t_s^h$  is the difference between the current time when the routing decision is being made  $t_{current}$  and the time when the packet is created at the source node  $t_{create}$ , i.e.,<sup>3</sup>

$$t_s^h = \max\{t_{min}, t_{current} - t_{create}\} \tag{4}$$

where  $t_{min}$  denotes the time of delivering a data packet over one hop.

The main problem that will be solved by DHGR can be summarized as follows: *Given the global parameter  $T_{QoS}$  and the current node’s local information (i.e.,  $t_s^h$  and  $P_h$ ), find an efficient distributed mechanism for adjusting  $\alpha$  to achieve an end-to-end delay as close to  $T_{QoS}$  as possible in the long-term perspective.*

##### B. Reference-Value-Based $\alpha$ Adjustment: DHGR-I

We first consider a simple reference-value-based  $\alpha$  adjustment method, where  $\alpha$  is initially set to a reference value (e.g.,  $\alpha = 0$ ). The reference value can empirically be selected for a specific application.

Let  $T_s^h$  be the standard (or reference) time that can be used for delivering a packet from  $s$  to  $h$ , assuming that the total delay requirement  $T_{QoS}$  is satisfied. Then, the allowable delay for advancing the packet over distance  $P_h$  is estimated by

$$T_s^h = \left( \frac{P_h}{D_s^t} \right) \cdot T_{QoS}. \tag{5}$$

Recall that  $t_s^h$  is the actual delay that was experienced by the packet. If  $t_s^h > T_s^h$ , the experienced delay exceeds the allowable delay. We need to speed up data forwarding by increasing  $\alpha$ . We take a threshold-based approach for  $\alpha$  adjustment. If  $t_s^h$  is larger than  $T_s^h$  by a certain threshold (denoted by  $TH_{debit}^I$ ),  $\alpha$  will be updated as  $\alpha' = \alpha + \beta$ , where  $\beta$  is a predetermined constant. Then, as illustrated in Fig. 4,  $h$  deletes the current next-hop node for the flow, and a new next-hop node  $j$  is selected according to  $\alpha'$ , which is determined based on the criterion in (1). The opposite process is performed if  $t_s^h$  is less than  $T_s^h$  by more than a certain threshold  $TH_{credit}^I$ . Note that, if  $TH_{debit}^I$  is set to a smaller value (with a minimum of 0), the end-to-end delay will be guaranteed with a higher probability.

HGR with reference-value-based  $\alpha$  adjustment is denoted by DHGR-I. The pseudocode of DHGR-I is shown in Table III, where “←” denotes an assignment operation.

<sup>3</sup>We assume that the sensor clocks are synchronized to compute the delay and that  $t_{create}$  is carried in the packet. Many synchronization schemes that were proposed for WSNs can be adopted for this purpose [29].

TABLE III  
PSEUDOCODE FOR THE DATA-DISSEMINATION ALGORITHM  
WITH THE REFERENCE-VALUE-BASED  $\alpha$  ADJUSTMENT

```

procedure process_data(DATA( $\alpha, T_{QoS}, p, \alpha, s, t, hc_s^p, SeqNum$ ))
begin
00 Calculate  $t_s^h$  and  $T_s^h$ ; //Defined in Eqns.(4) and (5)
01 if ( $t_s^h - T_s^h$ ) >  $TH_{debit}^I$  then
02    $\alpha' \leftarrow \alpha + \beta$ ;
03   Update the next hop;
04 else if ( $T_s^h - t_s^h$ ) >  $TH_{credit}^I$  then
05    $\alpha' \leftarrow \alpha - \beta$ ;
06   Update the next hop;
07 endif
08  $p \leftarrow h$ ;
09  $hc_s^p \leftarrow hc_s^p + 1$ ;
10 Forward DATA( $p, s, t, hc_s^p, SeqNum$ ) to the next hop node
end

```

$s, t, p$  and  $h$ : identifiers of the source, the sink,  
the upstream node and the current node, respectively;  
 $hc_s^p$ : hop count from  $s$  to  $p$ ;  
 $SeqNum$ : sequence number of the data packet;

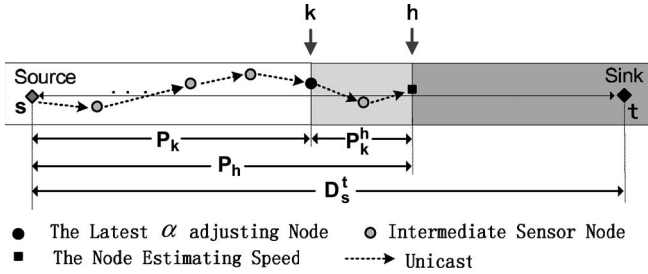


Fig. 5. Calculating speed along the path segment.

### C. Speed-Based $\alpha$ Adjustment Strategy: DHGR-II

Although the reference-value-based adjustment method is simple, the improper setting of the initial  $\alpha$  value may negatively affect the performance. In this section, we propose a method that is virtually independent of the initial  $\alpha$  value that was set by the source. Instead of keeping the reference  $\alpha$  fixed all the time as in *DHGR-I*, it will be updated at subsequent hops by considering the delay bound whenever needed. To more accurately adjust  $\alpha$  to meet the QoS objectives, a speed prediction model will be adopted.

The speed of a packet that arrives at an intermediate node  $h$  depends on the delay that it experiences. Here, we measure the distance from the previous node where the latest  $\alpha$  adjustment has been made. In Fig. 5,  $k$  denotes the node that most recently adjusts the  $\alpha$  value,  $h$  denotes the current node where the speed is being estimated,  $P_k$  and  $P_h$  denote the projected progress toward the sink at nodes  $k$  and  $h$ , respectively, and  $P_k^h$  denotes the projected progress along the path segment between  $k$  and  $h$ . It follows that  $P_k^h = P_h - P_k$ .

Let  $t_s^k$  and  $t_s^h$  be the delays from the source to nodes  $k$  and  $h$ , respectively. The speed along the path segment  $P_k^h$  is not adjusted; thus, the average speed along the path segment between  $k$  and  $h$ , which is denoted by  $v_k^h$ , can be calculated as

$$v_k^h = \frac{P_k^h}{t_s^h - t_s^k}. \quad (6)$$

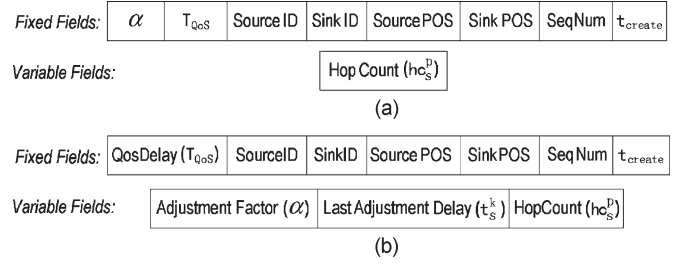


Fig. 6. Data packet formats. (a) DHGR-I. (b) DHGR-II.

$v_k^h$  is considered the current speed that was estimated by node  $h$ . Then, according to the speed, node  $h$  can predict whether the packet will arrive at the sink within the delay bound and if it continues to travel at the current speed. Node  $h$  adjusts the  $\alpha$  value as follows.

- 1) Let  $\tau_h^t$  be the expected latency from node  $h$  to the destination  $t$  using the current speed. Then,  $\tau_h^t$  can be calculated as  $\tau_h^t = (D_s^t - P_h)/v_k^h$ .
- 2) Let  $T_h^t$  be the time credit that was left at node  $h$ , which can be calculated as  $T_h^t = (D_s^t - P_h)/D_s^t \cdot T_{QoS}$ .
- 3) When  $\tau_h^t$  goes above a threshold (the higher threshold, denoted by  $TH_{debit}^{II}$ ), the packet is likely to miss the delay bound if its progress continues at the current estimated speed, and a decision for increasing  $\alpha$  is made to speed up the packet delivery.

The increased value is set to be proportional to the gap between  $\tau_h^t$  and  $T_h^t$ , e.g.,  $\sqrt{(\tau_h^t - T_h^t)/TH_{debit}^{II}}$ ; otherwise, node  $h$  decreases  $\alpha$  to slow down the speed. By instrumenting this speed adjustment, suboptimal localized decisions can globally be compensated as the packet travels between the source and the sink.

The packet formats in the two schemes are shown in Fig. 6. Compared with *DHGR-I*, the packet format in *DHGR-II* includes the following two additional variable packet fields: 1)  $\alpha$  and 2)  $t_s^k$ . The pseudocode of the *DHGR-II* scheme is described in Table IV.

## V. DYNAMIC HYBRID GEOGRAPHIC ROUTING DELAY ANALYSIS

### A. Concept of “Credit Delay” and “Debit Delay”

When node  $h$  at hop  $k$  receives a data packet with a particular  $\alpha$  value,  $t_s^h$  and  $T_s^h$  are calculated according to (4) and (5), respectively. It is not realistic to expect that  $t_s^h$  is exactly equal to  $T_s^h$ . Thus, upon the reception of data packet at node  $h$ , we have the following two cases.

- 1)  $t_s^h < T_s^h$ : The required delay is partially satisfied in the path segment from the source node to the current node in the viewpoint of  $h$ . In addition, an extra “credit delay” (i.e.,  $T_s^h - t_s^h$ ) is available, which is denoted by  $t_k^{c1}$  in Fig. 7. Note that the higher the speed, the larger the consumed energy. Thus, to save energy, node  $h$  is allowed to more slowly forward a data packet than the current speed by consuming credit delay  $t_k^{c1}$ . Initially, there is no credit delay available at the source node, i.e.,  $t_0^{c1} = 0$ .

TABLE IV  
PSEUDOCODE FOR THE DATA-DISEMINATION ALGORITHM  
WITH THE SPEED-BASED  $\alpha$  ADJUSTMENT

```

procedure process_data(DATA( $\alpha, T_{QoS}, k, t_s^k, p, t, hc_s^p, SeqNum$ ))
begin
00 Calculate  $v_k^h, \tau_h^t$ , and  $T_h^t$ 
01 if  $(\tau_h^t - T_h^t) > TH_{debit}^{II}$  then
02    $\alpha = \alpha + \sqrt{(\tau_h^t - T_h^t) / TH_{debit}^{II}}$ ;
03    $k \leftarrow h$ ;
04    $t_s^k \leftarrow t_s^h$ ;
05 else if  $(T_h^t - \tau_h^t) > TH_{credit}^{II}$  then
06    $\alpha = \alpha - \sqrt{(\tau_h^t - T_h^t) / TH_{credit}^{II}}$ ;
07    $k \leftarrow h$ ;
08    $t_s^k \leftarrow t_s^h$ ;
09 endif
10  $p \leftarrow h$ ;
11  $hc_s^p \leftarrow hc_s^p + 1$ ;
12 Select Next Hop Node According to  $\alpha$ ;
13 Forward DATA( $\alpha, k, t_s^k, p, t, hc_s^p, SeqNum$ ) to the selected
    next hop node;
end

```

$v_k^h$ : average speed along the path segment between  $k$  and  $h$ .  
If  $TH_{debit}^{II} = 0$ , the end-to-end delay requirement can be guaranteed with a very high possibility.

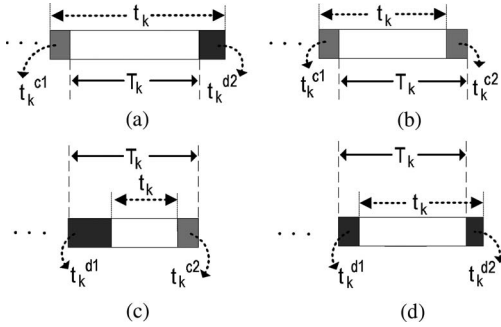


Fig. 7. Change of credit–debit delay from hop  $k$  to hop  $k+1$ . (a) “Credit” switches to “debit.” (b) No credit–debit change. (c) “Debit” switches to “credit.” (d) No debit–credit change.

- 2)  $t_s^h > T_s^h$ : The experienced delay exceeds the expected delivery time at node  $h$ . We address this issue by compensating for the “debit delay” at node  $h$ , which is denoted by  $t_k^{d1}$  and is equal to  $t_s^h - T_s^h$ . If such a tendency cannot be continuously reversed in the following hop(s), the delay bound would be hard to satisfy. Thus, node  $h$  intends to increase the data-forwarding speed to amortize the “debit delay.”

After the data transmission by node  $h$ , the following two cases are still possible: 1) “credit delay after the current hop” (denoted by  $t_k^{c2}$ ) and 2) “debit delay after the current hop” (denoted by  $t_k^{d2}$ ). If we consider the two cases when  $h$  receives the data packet and the other two cases after  $h$  transmits the packet, there are four combinations, as shown in Fig. 7. In particular, Fig. 7(a) and (c) represent the credit–debit relation changes in a single hop, whereas Fig. 7(b) and (d) indicate that the credit–debit relation does not change.

If we consider the entire path from the source to the sink, the goal of  $\alpha$  tuning is that the accumulated delay of data packets that arrive at the sink node should be less than and close to the  $T_{QoS}$  bound. However, from the viewpoint of a single node, it is

unnecessary to precisely adjust  $\alpha$  (or speed). Rather, the speed at node  $h$  does not need to be adjusted, as long as the following two cases happen.

- 1) Its credit delay  $t_k^{c1}$  is smaller than a certain threshold, e.g.,  $TH_{credit}$ . Otherwise, node  $h$  will decrease  $\alpha$  to consume its credit delay for energy saving.
- 2) Its debit delay  $t_k^{d1}$  is smaller than a certain threshold, e.g.,  $TH_{debit}$ . Otherwise, node  $h$  will increase  $\alpha$  to amortize the debit delay.

## B. DHGR Delay Analysis

Let  $T_k$  be the reserved delay credit for hop  $k$ , which is calculated according to the current speed and the projected progress from hop  $k$  to hop  $k+1$ , i.e.,  $T_k = (P_k^{k+1}/P_s^k) \cdot T_{QoS}$ . Let  $H$  be the number of hops along the path between the source and the sink. We have  $T_{QoS} = \sum_{k=0}^{H-1} T_k$ . Let  $t_k$  denote the delay that was experienced from the  $k$ th hop to the  $(k+1)$ th hop. Then,  $t_k$  in the four cases in Fig. 7 can be calculated as

$$t_k = \begin{cases} T_k + t_k^{c1} + t_k^{d2}, & \text{Fig. 7(a)} \\ T_k + t_k^{c1} - t_k^{c2}, & \text{Fig. 7(b)} \\ T_k - t_k^{d1} - t_k^{c2}, & \text{Fig. 7(c)} \\ T_k - t_k^{d1} + t_k^{d2}, & \text{Fig. 7(d)}. \end{cases} \quad (7)$$

Consider Fig. 7(a). The end-to-end packet delay  $T_{ete}$  can be calculated as

$$\begin{aligned}
 T_{ete} &= \sum_{k=0}^{H-1} t_k \\
 &= \sum_{k=0}^{H-1} (T_k + t_k^{c1} + t_k^{d2}) \\
 &= \sum_{k=0}^{H-1} T_k + \sum_{k=0}^{H-1} t_k^{c1} + \sum_{k=0}^{H-1} t_k^{d2} \\
 &= \sum_{k=0}^{H-1} T_k + t_0^{c1} + \sum_{k=1}^{H-1} t_k^{c1} + \sum_{k=0}^{H-1} t_k^{d2} \\
 &= T_{QoS} + 0 - \sum_{k=1}^{H-1} t_{k-1}^{d2} + \sum_{k=0}^{H-1} t_k^{d2} \\
 &= T_{QoS} - \sum_{k=0}^{H-2} t_k^{d2} + \sum_{k=0}^{H-1} t_k^{d2} \\
 &= T_{QoS} + t_{H-1}^{d2} = T_{QoS} - t_{H-1}^{c2}. \quad (8)
 \end{aligned}$$

$t_k^{c1}$  can be considered as the negative “debit delay” from its previous hop; thus, we have  $t_k^{c1} = -t_{k-1}^{d2}$  during the calculation of (8). In (7), the credit delay can also be regarded as the negative debit delay, i.e.,  $t_k^{c1} = -t_k^{d1}$ , and  $t_k^{c2} = -t_k^{d2}$ . Thus, the other three cases in Fig. 7 can similarly be handled as Fig. 7(a) according to (7) and (8).

Next, the maximum credit delay during the current data transmission will be derived. We consider the worst case at the  $k$ th hop. Assuming that  $t_k^{c1}$  is very close to  $TH_{credit}$  but is still less than  $TH_{credit}$ , node  $h$  at hop  $k$  will not control the speed. We further assume that the uncontrolled speed at node  $h$  is the

fastest one.<sup>4</sup> Then, after data delivery at hop  $k$ ,  $t_k^{c2}$  reaches its maximum value, which is given by

$$\begin{aligned} \max \{t_k^{c2}\} &= \max \{t_k^{c1} + T_k - t_k\} \\ &= \max \{t_k^{c1}\} + \max\{T_k\} - \min\{t_k\} \\ &< TH_{credit} + R/D_s^t \cdot T_{QoS} - t_{\min} \\ &\text{for } k = 1, 2, \dots, H - 1 \end{aligned} \quad (9)$$

where  $R$  denotes the maximum transmission range, and  $t_{\min}$  denotes the minimum hop delay.

To calculate the maximum debit delay after node  $h$  forwards the data packet, we consider the other worst case. Similarly, assume that  $t_k^{d1}$  is very close to  $TH_{debit}$  but is still less than  $TH_{debit}$ . Then, node  $h$  will keep the current speed. Assuming that the speed is the slowest at this moment, then  $t_k^{d2}$  will be increased to its maximum value, i.e.,

$$\begin{aligned} \max \{t_k^{d2}\} &= \max \{t_k^{d1} + t_k - T_k\} \\ &< \max \{t_k^{d1}\} + \max\{t_k\} - \min\{T_k\} \\ &< TH_{debit} + t_{\max} \\ &\text{for } k = 1, 2, \dots, H - 1. \end{aligned} \quad (10)$$

In (10),  $t_{\max}$  denotes the maximum hop delay, and  $T_k$  will be close to 0 in the case that the projected progress is close to 0 at hop  $i$ .

According to (8)–(10), we can calculate the minimum and maximum of  $T_{ete}$  when the perfect DHGR scheme is employed, i.e.,<sup>5</sup>

$$\begin{cases} \min\{T_{ete}\} = T_{QoS} - \max \{t_{H-1}^{c2}\} \\ \quad = \frac{D_s^t - R}{D_s^t} \cdot T_{QoS} + t_{\min} - TH_{credit} \\ \max\{T_{ete}\} = T_{QoS} + \max \{t_{H-1}^{d2}\} \\ \quad = T_{QoS} + t_{\max} + TH_{debit}. \end{cases} \quad (11)$$

The range of  $T_{ete}$  is thus  $\min\{T_{ete}\} < T_{ete} < \max\{T_{ete}\}$ .

### C. Validation of the DHGR Delay Analysis

In (8), it can be observed that the credit and debit are compensated in a long-term view, with  $t_s^h$  converging to  $T_{QoS}$  as the packet approaches the sink node. To validate the range of  $T_{ete}$  that was derived in (11), we vary  $T_{QoS}$  from 0.7 s to 1.1 s and compare  $\min\{T_{ete}\}$  and  $\max\{T_{ete}\}$ , as predicted from the aforementioned analysis with the *DHGR-II* simulation results. Given the scenario in Section VI, Fig. 8 shows the simulated delay results of *DHGR-II* and illustrates HGR’s adaptability to an application-specific  $T_{QoS}$ .

Let  $T^\downarrow$  be the delay in the pure distance-based scheme, whereas  $T^\uparrow$  denotes the delay in the pure direction-based scheme. Then,  $[T^\downarrow, T^\uparrow]$  is considered the *scope of adjustment* in DHGR. As shown in Fig. 8, within the scope of adjustment, the resulting  $T_{ete}$  of *DHGR-II* is in accordance with the analysis results.

<sup>4</sup>That is, when  $T_k$  reaches its maximum value, the maximum reserved delay credit is calculated based on the maximum projected progress of  $R$ . Then, we have  $\max\{T_k\} = R/D_s^t \cdot T_{QoS}$ .

<sup>5</sup>If  $TH_{debit}$  is equal to  $-t_{\max}$ , then  $\max\{T_{ete}\} = T_{QoS} \Rightarrow T_{ete} \leq T_{QoS}$ .

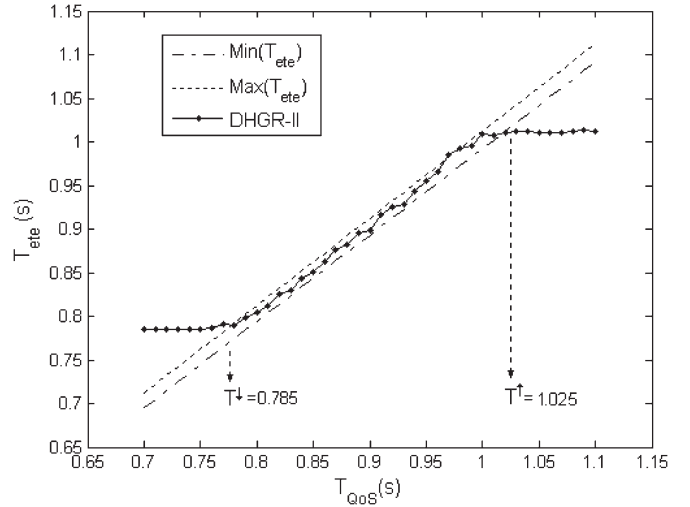


Fig. 8. Impact of  $T_{QoS}$  on  $\min\{T_{ete}\}$ ,  $\max\{T_{ete}\}$  and adjusted delay in *DHGR-II*, with  $TH_{debit} = 0$  (ms),  $TH_{credit} = 7.5$  (ms),  $t_{\min} = 7$  (ms) and  $t_{\max} = 7.5$  (ms).

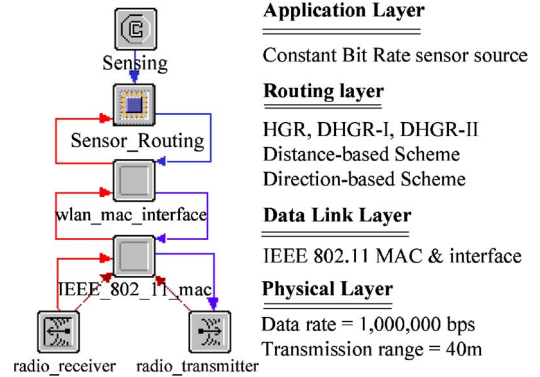


Fig. 9. Sensor node model that was used in the simulations.

## VI. PERFORMANCE EVALUATION

To evaluate the performance of the proposed schemes, we compare *HGR*, *DHGR-I*, and *DHGR-II* with a representative distance-based scheme (e.g., GFG [6], [7] or greedy perimeter stateless routing (GPSR) [8]) and a representative direction-based scheme (e.g., compass routing (CR) [9]) using extensive simulation studies. We first present our simulation settings and performance metrics in Section VI-A. The simulation results are presented and discussed in Section VI-B.

### A. Simulation Methodology

We implement our protocols and perform simulations using the OPNET Modeler [30]. The WSN network consists of 2500 nodes that were uniformly deployed in a 2000 m × 500 m field. Similar to [31], we let one sink stay at a corner of the field and one source node be located at the diagonal corner. Our sensor node implementation is illustrated in Fig. 9, which has a four-layer protocol structure. The sensor application module consists of a constant-bit-rate source, which generates sensed data every 1 s (2 kB each). Similar to [5], we use the IEEE 802.11 distributed coordination function (DCF) as the underlying MAC, and the radio transmission range ( $R$ ) is set to 40 m (if not specified otherwise). The data rate of the wireless channel is 1 Mb/s.

Similar to [21] and [31], each node can adjust its transmit power to reach a given distance within  $R$  instead of always using the maximum transmit power. We assume that both the sink and sensor nodes are stationary.  $TH_{debit}$  and  $TH_{credit}$  are set to a default value of 0 and 7.5 ms, respectively.  $\alpha$  is initially set to 0 by the source in *DHGR-II*.

The following performance metrics are evaluated during the simulations.

- 1) *Average end-to-end delay  $T_{ete}$* . This includes all the delay elements during packet transmissions, e.g., queuing delays, retransmission delays due to collision at the MAC layer, and packet transmission delays.
- 2) *Normalized average end-to-end delay  $T_{ete}^n$* . This is defined as  $T_{ete}/T_{QoS}$ . If  $T_{ete}^n > 1$ , the delay requirement is violated.
- 3) *Energy consumption per successful data delivery  $E$* . This is the ratio of network energy consumption to the number of data packets that were successfully delivered to the sink. The network energy consumption includes all the energy that was consumed by transmitting, receiving, and overhearing during a simulation. Similar to [32], we do not account for energy consumption in the idle state, because this part is approximately the same for all the schemes that were simulated. In addition, the transmission power of each node is modeled to be distance sensitive, because we assume that the nodes in the network can adjust their transmission ranges, depending on how far they need/choose to transmit.

In all the figures in this section, each data point is the average of 45 simulations with different random seeds.

**B. Simulation Results and Evaluations**

1) *Performance Comparison With Varying Maximum Transmission Range*: In the following sets of simulation results, node density is changed by varying  $R$  from 100 m to 250 m. HGR results are obtained using various fixed  $\alpha$  values.

In Fig. 10, the delays of all the schemes decrease as  $R$  is increased. The larger  $R$  is, the smaller the hop counts are, and the lower the obtained delay becomes. On the other hand, given a fixed  $R$ , the delays of HGR lies in between those of the distance- and the direction-based schemes. HGR behaves more like the distance-based scheme when a larger fixed  $\alpha$  value is set. The direction-based scheme has the largest delays, because it only considers the directions while ignoring packet progress. Although smaller Euclidean path lengths are obtained in the direction-based scheme, it introduces larger numbers of hops and, thus, longer delays.

Fig. 11 shows that the energy consumptions of all the schemes increase as  $R$  is increased. The larger  $R$  is, the longer the hop distance becomes. Given a fixed  $R$ , the energy consumption of the distance-based scheme is always larger than both HGR and the direction-based scheme. The distance-based scheme tries to maximize packet progress by using a larger hop distance and Euclidean path length, and thus, it consumes more energy than the other two schemes, which consider directions during next-hop selections. Although the energy consumption of HGR is larger than that of the direction-based scheme,

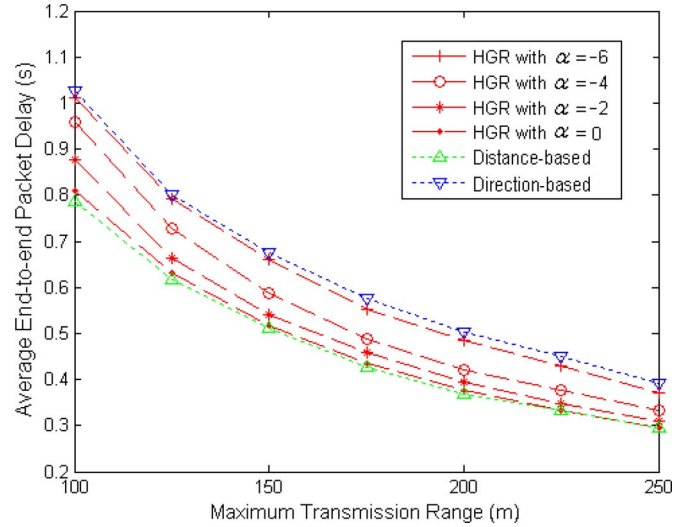


Fig. 10. Impact of  $R$  on the average end-to-end delay.

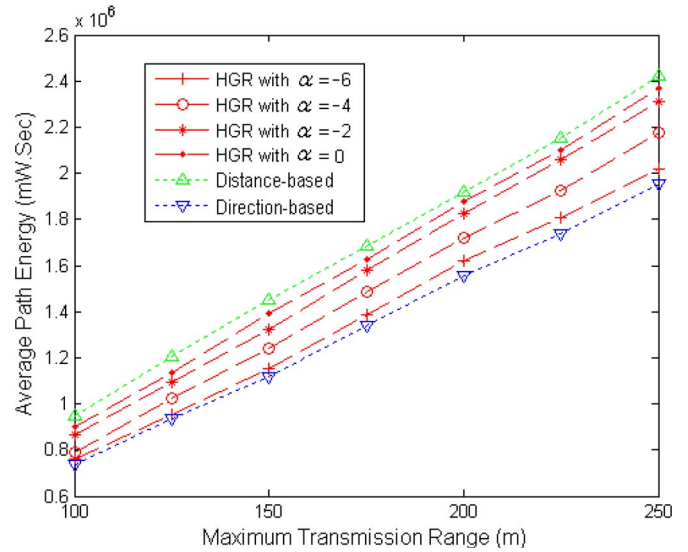


Fig. 11. Impact of  $R$  on energy consumption per successful data delivery.

the delay of HGR is smaller than that of the direction-based scheme.

In Figs. 10 and 11, it can be observed that, by adjusting  $\alpha$ , HGR can achieve a good tradeoff between the average delay and power consumption. In particular, HGR always yields lower delay than the direction-based scheme and lower power consumption compared with the distance-based scheme.

2) *Performance Comparison With Varying Delay Objectives*: In the following sets of results, the delay requirement  $T_{QoS}$  is varied from 0.7 s to 1.1 s, and we set three reference values for  $\alpha$  for *DHGR-I*. Given a fixed reference  $\alpha$ , *DHGR-I* adaptively adjusts  $T_{ete}$  to meet the specified  $T_{QoS}$ . In Figs. 12 and 14, it is shown that the delay and energy consumption of both the distance and direction-based schemes are not affected by  $T_{QoS}$  or the reference  $\alpha$ .

As shown in Figs. 12–14, the chosen reference  $\alpha$  value in *DHGR-I* has a big impact on its performance. The lower the reference  $\alpha$  value is, the closer the respective performance curves of *DHGR-I* are to the corresponding curves of the

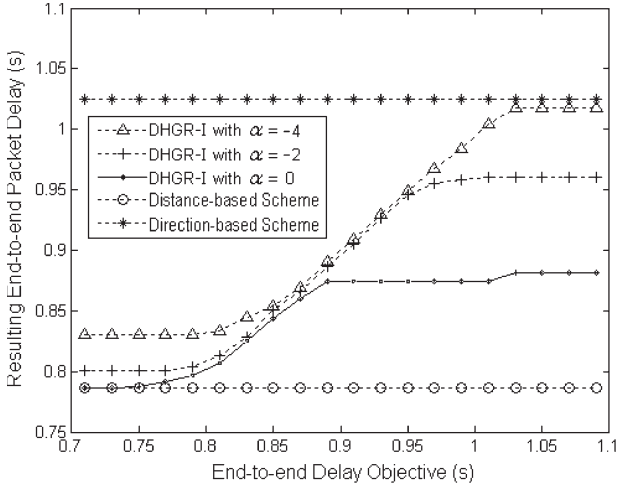


Fig. 12. Impact of  $T_{QoS}$  on the end-to-end delay that was achieved by *DHGR-I*.

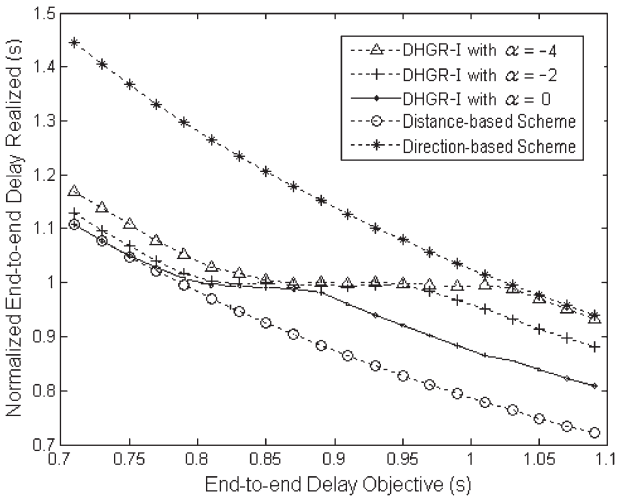


Fig. 13. Impact of  $T_{QoS}$  on the normalized end-to-end delay that was achieved by *DHGR-I*.

direction-based scheme at high  $T_{QoS}$  values. Conversely, the higher the reference  $\alpha$  value is, the closer the respective performance curves of *DHGR-I* are to the corresponding curves of the distance-based scheme at low  $T_{QoS}$  values. Fig. 13 shows the curves of  $T_{ete}^n$  for the schemes. The distance-based scheme satisfies the required delay if  $T_{QoS} > 0.785s$ , *DHGR-I* with  $\alpha = 0, -2, -4$  satisfies the average delay if  $T_{QoS} > 0.79, 0.82, 0.85s$ , respectively, and the direction-based scheme satisfies the average delay if  $T_{QoS} > 1.025s$ . Then, in terms of the average delay guarantees, the decreasing order of QoS support is given as follows:

- 1) distance-based scheme;
- 2) *DHGR-I* with  $\alpha = 0$ ;
- 3) *DHGR-I* with  $\alpha = -2$ ;
- 4) *DHGR-I* with  $\alpha = -4$ ;
- 5) direction-based scheme.

In Fig. 14, when  $T_{QoS}$  changes, the energy consumption of all the schemes exhibits exactly the reverse tendency for the delays in Fig. 12. Although the energy consumption of the direction-based scheme is always the lowest, its ability to satisfy a small

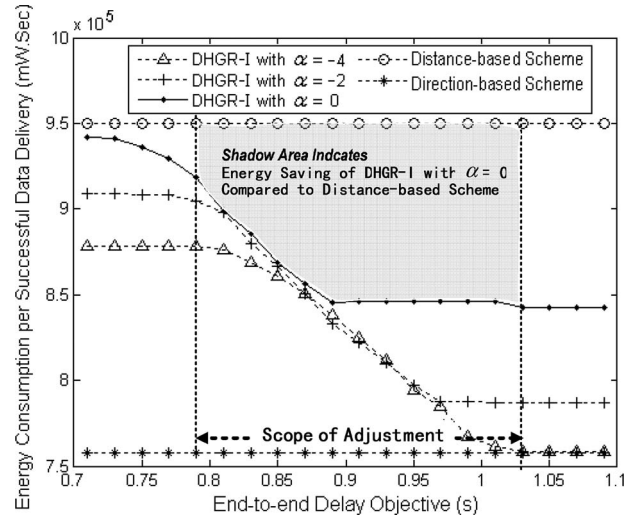


Fig. 14. Impact of  $T_{QoS}$  on the energy consumption per successful data delivery in *DHGR-I*.

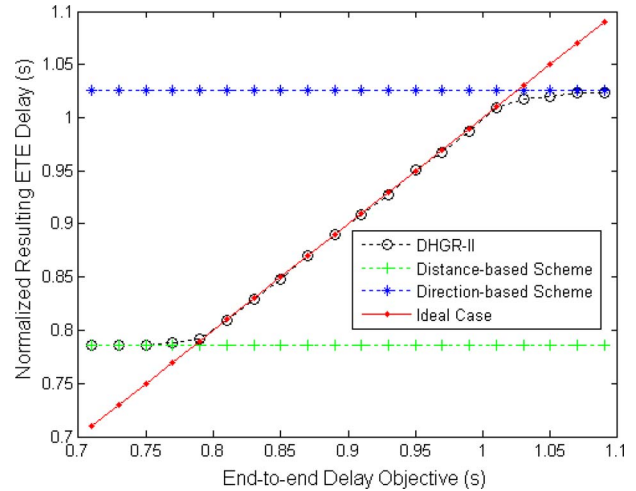


Fig. 15. Impact of  $T_{QoS}$  on the end-to-end delay that was achieved by *DHGR-II*.

delay constraint is the lowest. In comparison, *DHGR-I* achieves a more efficient tradeoff between delay guarantees and energy consumption than both the distance- and the direction-based schemes.

In Fig. 15, the solid line represents the ideal case, where  $T_{ete}$  of *DHGR-II* perfectly tracks  $T_{QoS}$ . It is shown that the *DHGR-II* delay curve is very close to that of ideal case, whereas the curves in the distance- and the direction-based schemes are unresponsive to changes in  $T_{QoS}$ . Both the distance-based scheme and *DHGR-II* can satisfy the average delay constraint if  $T_{QoS}$  is larger than the delay's lower junction, as shown in Fig. 16. However, *DHGR-II* has lower energy consumption than the distance-based scheme, as shown in Fig. 17.

3) *Integrated Performance Comparison*: As mentioned in Section V-B,  $T_{ete}$  can only be adjusted between  $T^\downarrow$  and  $T^\uparrow$ . Let  $T_{gpsr}$  represent the  $T_{ete}$  of the distance-based scheme and  $T_{cr}$  represent the  $T_{ete}$  of the direction-based scheme. Then,  $T^\downarrow = T_{gpsr}$ , and  $T^\uparrow = T_{cr}$ . Let  $T_{gpsr}^n$  and  $T_{cr}^n$  be the normalized  $T_{gpsr}$  and  $T_{cr}$ , respectively. In Fig. 16, the curve

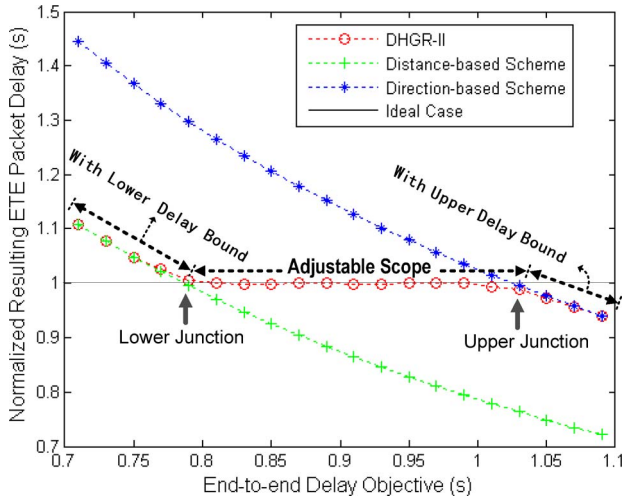


Fig. 16. Impact of  $T_{QoS}$  on the normalized end-to-end delay that was achieved by *DHGR-II*.

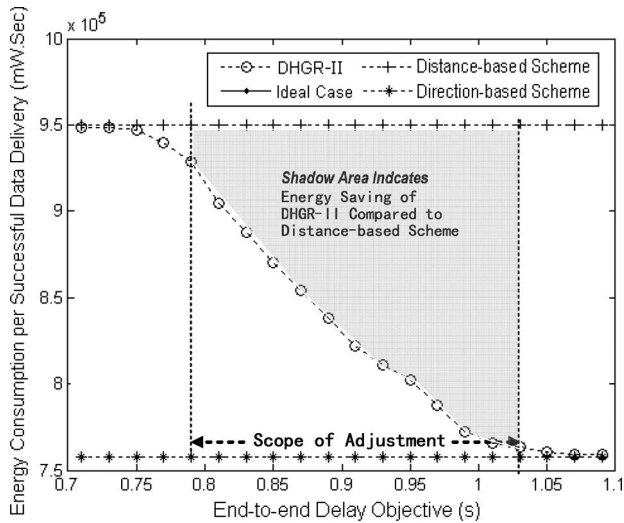


Fig. 17. Impact of  $T_{QoS}$  on the energy consumption per successful data delivery in *DHGR-II*.

of  $T_{gpsr}^n$  crosses the ideal curve at *LowerJunction*, whereas the curve of  $T_{cr}$  crosses the ideal curve at *UpperJunction*. A better adjustment algorithm should make the resulting  $T_{ete}$  curve closer to the line that connects *LowerJunction* and *UpperJunction* (the scope of adjustment), i.e., satisfy the required QoS while minimizing energy consumption. Let  $L_{overlap}$  be the ratio of a resulting  $T_{ete}$  curve that overlapped with the ideal curve by a 98% confidence within the scope of adjustment. Let  $r_{QoS}$  denote the ratio of meeting the delay constraint by a 98% confidence over the scope of adjustment. Let  $E_{saving}$  be the accumulated energy saving of *DHGR-I* and *DHGR-II* compared to the distance-based scheme over the scope of adjustment, which corresponds to the shadowed areas in Figs. 14 and 17.

For time-sensitive applications over energy-constrained WSNs, it is important to consider both  $r_{QoS}$  and  $E_{saving}$ . We adopt the following metric (which is denoted by  $\eta$ ) to evaluate the integrated performance in terms of meeting delay constraints and energy saving:

$$\eta = r_{QoS} \cdot E_{saving}. \tag{12}$$

TABLE V  
PERFORMANCE OF SATISFYING DELAY CONSTRAINTS AND ENERGY SAVING

Scheme	$L_{overlap}$	$r_{QoS}$	$E_{saving}$	$\eta$
Distance-based:	0%	99.5%	0	0
Direction-based:	0%	0.5%	$4.62 \times 10^6$	0
<i>DHGR-I</i> ( $\alpha=0$ ):	25.2%	66.4%	$2.18 \times 10^6$	$1.44 \times 10^6$
<i>DHGR-I</i> ( $\alpha=-2$ ):	52.8%	85.9%	$2.87 \times 10^6$	$2.47 \times 10^6$
<i>DHGR-I</i> ( $\alpha=-4$ ):	66.4%	91.6%	$3.08 \times 10^6$	$2.83 \times 10^6$
<i>DHGR-II</i> :	100%	100%	$2.88 \times 10^6$	$2.88 \times 10^6$

The higher  $\eta$  is, the better the composite performance becomes, which was provided by the WSN to energy efficiently support time-constrained services. Table V shows a comparison of the schemes in terms of  $L_{overlap}$ ,  $r_{QoS}$ ,  $E_{saving}$ , and  $\eta$ . The results in Table V show that *DHGR-II* has the highest  $\eta$ , and more importantly,  $\eta$  is proportional to  $L_{overlap}$ , which verifies that the precision of delay adjustment in *DHGR* can help in satisfying the average delay constraint while maximizing energy saving. Based on both  $\eta$  and  $L_{overlap}$ , we can get the same increasing order of performance in terms of the integrated eligibility level, i.e., the distance- or the direction-based scheme, *DHGR-I* with  $\alpha = 0$ , *DHGR-I* with  $\alpha = -2$ , and *HGR-I* with  $\alpha = -4$ , *DHGR-II*. Compared with *DHGR-I*, *DHGR-II* is virtually independent of the initial  $\alpha$  setting and has a better integrated performance. Although *DHGR-II* has higher complexity than *DHGR-I*, the  $\alpha$  adjustment scheme in *DHGR-II* is more efficient. This result also illustrates the tradeoff between complexity and efficiency of the two *DHGR* algorithms in this paper.

### VII. CONCLUSION

This paper has proposed a novel HGR protocol that was designed to achieve an efficient tradeoff between energy efficiency and delay performance. HGR employs a novel hybrid criterion based on direction and distance to evaluate the eligibility of neighboring nodes as the next-hop relay. Furthermore, a weight factor has been introduced to weigh the impact of direction and distance on the HGR operation. Two novel adjustment strategies *DHGR-I* and *DHGR-II* have been proposed to satisfy the end-to-end average packet delay constraint while maximizing energy saving. An analysis has been given to bound the end-to-end delays of the HGR schemes. Extensive simulations show that the HGR schemes can achieve a flexible tradeoff between delay and energy.

### REFERENCES

- [1] J. Al-Karaki and E. Kamal, "Routing techniques in wireless sensor networks: A survey," *IEEE Pers. Commun.*, vol. 11, no. 6, pp. 6–28, Dec. 2004.
- [2] S. Mao and Y. T. Hou, "BeamStar: An edge-based approach to routing in wireless sensor networks," *IEEE Trans. Mobile Comput.*, vol. 6, no. 11, pp. 1284–1296, Nov. 2007.
- [3] A. Boukerche, X. Cheng, and J. Linus, "Energy-aware data-centric routing in microsensor networks," in *Proc. ACM MSWiM*, San Diego, CA, Sep. 2003, pp. 42–49.
- [4] A. Bukerche, I. Chatzigiannakis, and S. Nikolettseas, "Power-efficient data propagation protocols for wireless sensor networks," *Simulation*, vol. 81, no. 6, pp. 399–411, Jun. 2005.

- [5] C. Intanagonwiwat, R. Govindan, and D. Estrin, "Directed diffusion: A scalable and robust communication paradigm for sensor networks," in *Proc. ACM MobiCom*, Boston, MA, Aug. 2000, pp. 56–67.
- [6] P. Bose, P. Morin, I. Stojmenovic, and J. Urrutia, "Routing with guaranteed delivery in ad hoc wireless networks," in *Proc. ACM DIAL*, Seattle, WA, Aug. 1999, pp. 48–55.
- [7] H. Frey and I. Stojmenovic, "On delivery guarantees of face and combined greedy–face routing algorithms in ad hoc and sensor networks," in *Proc. ACM MobiCom*, Los Angeles, CA, Sep. 2006, pp. 390–401.
- [8] B. Karp and H. T. Kung, "GPSR: Greedy perimeter stateless routing for wireless networks," in *Proc. ACM MobiCom*, Boston, MA, Aug. 2000, pp. 243–254.
- [9] E. Kranakis, H. Singh, and J. Urrutia, "Compass routing on geometric networks," in *Proc. 11th CCCG*, Vancouver, BC, Canada, Aug. 1999, pp. 51–54.
- [10] S. Basagni, I. Chlamtac, V. R. Syrotiuk, and B. A. Woodward, "A distance routing effect algorithm for mobility (DREAM)," in *Proc. ACM MobiCom*, Dallas, TX, Oct. 1998, pp. 76–84.
- [11] T. He, J. Stankovic, C. Lu, and T. Abdelzaher, "SPEED: A stateless protocol for real-time communication in sensor networks," in *Proc. IEEE Int. Conf. Distrib. Comput. Syst.*, Providence, RI, May 2003, pp. 46–55.
- [12] E. Felemban, C.-G. Lee, and E. Ekici, "MMSPEED: Multipath multi-SPEED protocol for QoS guarantee of reliability and timeliness in wireless sensor networks," *IEEE Trans. Mobile Comput.*, vol. 5, no. 6, pp. 738–754, Jun. 2006.
- [13] I. Stojmenovic, "Position-based routing in ad hoc networks," *IEEE Commun. Mag.*, vol. 40, no. 7, pp. 128–134, Jul. 2002.
- [14] G. G. Finn, "Routing and addressing problems in large metropolitan-scale internetworks," *Inf. Sci. Inst.*, Marina del Rey, CA, Tech. Rep. ISI/RR-87-180, Mar. 1987.
- [15] M. Chen, V. Leung, S. Mao, and Y. Yuan, "Directional geographical routing for real-time video communications in wireless sensor networks," *Comput. Commun.*, vol. 30, no. 17, pp. 3368–3383, Nov. 2007.
- [16] M. Chen, V. Leung, S. Mao, and M. Li, "Cross-layer and path priority scheduling based real-time video communications over wireless sensor networks," in *Proc. IEEE VTC*, Marina Bay, Singapore, May 2008, pp. 2873–2877.
- [17] L. Shu, Y. Zhang, L. T. Yang, Y. Wang, M. Hauswirth, and N. Xiong, "TPGF: Geographic routing in wireless multimedia sensor networks," *J. Telecommun. Syst.*, to be published.
- [18] Y. Yuan, Z. K. Yang, Z. H. He, and J. H. He, "An integrated energy-aware wireless transmission system for QoS provisioning in wireless sensor networks," *Comput. Commun.*, vol. 29, no. 2, pp. 162–172, Jan. 2006.
- [19] M. Chen, T. Kwon, and Y. Choi, "Energy-efficient differentiated directed diffusion for real-time traffic in wireless sensor networks," *Comput. Commun.*, vol. 29, no. 2, pp. 231–245, Jan. 2006.
- [20] Crossbow Technol., San Jose, CA. [Online]. Available: <http://www.xbow.com>
- [21] L. Galluccio, A. Leonardi, G. Morabito, and S. Palazzo, "A MAC/routing cross-layer approach to geographic forwarding in wireless sensor networks," *J. Ad Hoc Netw.*, vol. 5, no. 6, pp. 872–884, Aug. 2007.
- [22] T. S. Rappaport, *Wireless Communications: Principles and Practice*. Indianapolis, IN: Prentice-Hall, 2002.
- [23] H. Takagi and L. Kleinrock, "Optimal transmission ranges for randomly distributed packet radio terminals," *IEEE Trans. Commun.*, vol. COM-32, no. 3, pp. 246–257, Mar. 1984.
- [24] M. Chen, X. Wang, V. Leung, and Y. Yuan, "Virtual coordinates-based routing in wireless sensor networks," *Sensor Lett.*, vol. 4, no. 3, pp. 325–330, Sep. 2006.
- [25] L. Zou, M. Lu, and Z. Xiong, "A distributed algorithm for the dead-end problem of location-based routing in sensor networks," *IEEE Trans. Veh. Technol.*, vol. 54, no. 4, pp. 1509–1522, Jul. 2005.
- [26] Q. Fang, J. Gao, and L. Guibas, "Locating and bypassing routing holes in sensor networks," in *Proc. IEEE INFOCOM*, Hong Kong, Mar. 2004, pp. 2458–2468.
- [27] A. Boukerche, R. Pazzi, and R. Araujo, "Fault-tolerant wireless sensor network routing protocols for the supervision of context-aware physical environments," *J. Parallel Distrib. Comput.*, vol. 66, no. 4, pp. 586–599, Apr. 2006.
- [28] M. Chen, V. Leung, S. Mao, and T. Kwon, "Receiver-oriented load-balancing and reliable routing in wireless sensor networks," *Wirel. Commun. Mobile Comput. J.*, vol. 9, no. 3, pp. 405–416, Mar. 2009.
- [29] B. Sundararaman, U. Buy, and A. D. Kshemkalyani, "Clock synchronization in wireless sensor networks: A survey," *Ad Hoc Netw.*, vol. 3, no. 3, pp. 281–323, May 2005.
- [30] *OPNET Modeler*. [Online]. Available: <http://www.opnet.com>
- [31] F. Ye, G. Zhong, S. Lu, and L. Zhang, "GRADient broadcast: A robust data delivery protocol for large-scale sensor networks," *ACM Wirel. Netw.*, vol. 11, no. 3, pp. 285–298, May 2005.
- [32] J. Gao and L. Zhang, "Load-balancing shortest path routing in wireless networks," in *Proc. IEEE INFOCOM*, Hong Kong, Mar. 2004, pp. 1098–1107.



**Min Chen** (M'08) received the Ph.D. degree in electrical engineering from the South China University of Technology, Guangzhou, China, in July 2004.

He was a Postdoctoral Fellow with Seoul National University, Seoul, Korea, for one and a half years. He then joined the Department of Computer Science, University of British Columbia (UBC), Vancouver, BC, Canada, as a Research Associate, in March 2009. For three years, he was a Postdoctoral Fellow with the Department of Electrical and Computer Engineering, UBC. He is currently an Assistant Professor with the School of Computer Science and Engineering, Seoul National University.

He serves as a Corresponding Guest Editor for several international journals, such as the *ACM/Springer Mobile Networks and Applications*, the *International Journal of Communication Systems*, the *International Journal of Sensor Networks*, and the *International Journal of Communication Networks and Distributed Systems*. He has published more than 50 technical papers. He is also the author of *OPNET Network Simulation* (Tsinghua University Press, 2004).

Dr. Chen has served as the Session Chair for several conferences, including the 2008 IEEE Vehicular Technology Conference (VTC), the Fifth International Conference on Heterogeneous Networking for Quality, Reliability, Security, and Robustness (QShine 2008), the 11th International Conference on Advanced Communication Technology (ICACT 2009), the Fifth International Conference on Testbeds and Research Infrastructures for the Development of Networks and Communities (TridentCom 2009), and the 2009 IEEE International Conference on Communications. He was the Technical Program Committee (TPC) Chair of the 2009 International Workshop on Advanced Sensor Integration Technology (ASIT) and a TPC Cochair of the First International Workshop on Pervasive Computing Systems and Infrastructures (PCSI 2009). He was the recipient of the Best Paper Runner-up Award at QShine 2008.



**Victor C. M. Leung** (S'75–M'89–SM'97–F'03) received the B.A.Sc. (Hons.) degree in electrical engineering in 1977 and the Ph.D. degree in electrical engineering, through the Natural Sciences and Engineering Research Council Postgraduate Scholarship Program, in 1981 from the University of British Columbia (UBC), Vancouver, BC, Canada.

From 1981 to 1987, he was a Senior Member of Technical Staff with MPR Teltech Ltd., specializing in the planning, design, and analysis of satellite communication systems. In 1988, he was a Lecturer with the Department of Electronics, Chinese University of Hong Kong, Sha Tin, Hong Kong. In 1989, he returned to UBC as a Faculty Member, where he is currently a Professor and the TELUS Mobility Research Chair in Advanced Telecommunications Engineering with the Department of Electrical and Computer Engineering and a Member of the Institute for Computing, Information, and Cognitive Systems. He has published more than 380 papers in journals and conference proceedings. His research interests include wireless networks and mobile systems.

Dr. Leung is a Fellow of the Engineering Institute of Canada and the Canadian Academy of Engineering and a Voting Member of the Association for Computing Machinery. He serves on the editorial boards of several journals, including the *IEEE TRANSACTIONS ON WIRELESS COMMUNICATIONS* and the *IEEE TRANSACTIONS ON COMPUTERS*. He has served on the Technical Program Committees (TPC) of numerous conferences. He was the TPC Vice Chair of the 2005 IEEE Wireless Communication Networking Conference, a General Cochair of the Eighth ACM/IEEE International Symposium on Modeling, Analysis, and Simulation of Wireless and Mobile Systems Symposium in 2005, the General Chair of the Fourth International Conference on Heterogeneous Networking for Quality, Reliability, Security, and Robustness in 2007, and the TPC Chair of the Wireless Networks and Cognitive Radio Track of the 68th IEEE Vehicular Technology Conference in the Fall of 2008. He was a General Cochair of the Seventh IEEE/IFIP International Conference on Embedded and Ubiquitous Computing in 2009. He received the Association of Professional Economists of British Columbia Gold Medal for being the head of the graduating class of the Faculty of Applied Science.



**Shiwen Mao** (S'99–M'04–SM'09) received the Ph.D. degree in electrical and computer engineering from Polytechnic University, Brooklyn, NY, in 2004.

From 1997 to 1998, he was a Research Member with the IBM China Research Laboratory, Beijing, China. In the summer of 2001, he was a Research Intern with Avaya Laboratories—Research, Holmdel, NJ. From 2003 to 2006, he was a Research Scientist with the Bradley Department of Electrical and Computer Engineering, Virginia Institute of Technology,

Blacksburg. He is currently an Assistant Professor with the Department of Electrical and Computer Engineering, Auburn University, Auburn, AL. He is on the editorial board of *Advances in Multimedia*, the *International Journal of Communication Systems*, the *Bentham Open Transportation Journal*, and the *ICST Transactions on Mobile Communications and Applications*. He is a coauthor of *TCP/IP Essentials: A Lab-Based Approach* (Cambridge University Press, 2004). His research interests include cognitive radio networks, cross-layer optimization of wireless networks, and multimedia communications.

Dr. Mao received the Leonard G. Abraham Prize in Communications Systems from the IEEE Communications Society in 2004 and the Best Paper Runner-up Award at the Fifth International Conference on Heterogeneous Networking for Quality, Reliability, Security, and Robustness in 2008.



**Yang Xiao** (S'98–M'01–SM'04) received the Ph.D. degree in computer science and engineering from Wright State University, Dayton, OH, in 2001.

He has been a Guest Professor with Jilin University, Changchun, China, and an Adjunct Professor with Zhejiang University, Hangzhou, China. He served in industry as a Medium Access Control Architect, working on the IEEE 802.11 standard enhancement, and then joined the Department of Computer Science, University of Memphis, Memphis, TN, in 2002. From 2001 to 2004, he was a Voting

Member of the IEEE 802.11 Working Group. He is currently on tenure with the Department of Computer Science, University of Alabama, Tuscaloosa. He is a Referee/Reviewer for several funding agencies, a Panelist for the U.S. National Science Foundation (NSF), and a Member of the Telecommunications Expert Committee, Canada Foundation for Innovation. He is the Editor-in-Chief of the *International Journal of Security and Networks*, the *International Journal of Sensor Networks*, and the *International Journal of Telemedicine and Applications*. He serves on the Technical Program Committees of more than 100 conferences such as the IEEE Conference on Computer Communications, the IEEE International Conference on Distributed Computing Systems, the ACM International Symposium on Mobile Ad Hoc Networking and Computing, the IEEE International Conference on Communications, the IEEE Global Telecommunications Conference, and the IEEE Wireless Communications and Networking Conference. He has published more than 300 papers in major journals, refereed conference proceedings, and book chapters. His research has been supported by the NSF, the U.S. Army Research, Fleet, and Industrial Supply Center, San Diego, and the Research Grants Committee, University of Alabama. His research interests include security, telemedicine, robots, sensor networks, and wireless networks.

Dr. Xiao is a member of the American Telemedicine Association. He is an Associate Editor for several journals, including the IEEE TRANSACTIONS ON VEHICULAR TECHNOLOGY.



**Imrich Chlamtac** (M'86–SM'86–F'93) received the B.Sci. and M.Sci. degrees in mathematics with Highest Distinction from Tel Aviv University, Tel Aviv, Israel, in 1977 and Ph.D. degree in computer science from the University of Minnesota, Minneapolis, in 1979.

He was with Technion—Israel Institute of Technology, Haifa, Israel, the University of Massachusetts, Amherst, and DEC Research. He helped found several successful technology firms, including Consip Ltd. and BCN Inc., which is

one of the largest system integrators in central Europe. He has held various chaired professorships in the U.S. and Europe, including the distinguished Chair in Telecommunications Professorship with the University of Texas at Dallas, Richardson; the Sackler Professorship with Tel Aviv University, Tel Aviv, Israel; the University Professorship with the Budapest University of Technology and Economics, Budapest, Hungary; and the Honorary Professorship with the Beijing University of Posts and Telecommunications, Beijing, China. He is currently the President of Create-Net, which is a nonprofit international research institute, and the Bruno Kessler Honorary Professor with the University of Trento, Trento, Italy. He is the founding Editor-in-Chief of the *ACM/Springer Wireless Networks* and the *ACM/Springer Journal on Special Topics in Mobile Networks and Applications*. He has published more than 400 refereed journal papers and conference proceedings and is listed among the Institute for Scientific Information's Highly Cited Researchers in Computer Science. He is a coauthor of several books, including *Local Area Networks* (1980), which is the first book on this topic, and the Amazon.com best seller *Wireless and Mobile Network Architectures* (Wiley).

Dr. Chlamtac is a Fellow of the Association for Computing Machinery (ACM). He has widely contributed to the scientific community's activities with the IEEE, ACM, and the International Society for Optical Engineers. More recently, he has been the Chair of the Scientific Council, Institute for Computer Sciences, Social-Informatics and Telecommunications Engineering (ICST). He is also the Founder and Chair of the ACM Sigmobility. He is the Founding Steering Committee Chair or the Chair of several leading conferences, including ACM Mobicom, ACM SigCom, and conferences that were cosponsored by ICST, Create-Net, and IEEE Societies, e.g., the International Conference on Broadband Communications, Networks, and Systems, the International Conference on Testbeds and Research Infrastructures for the Development of Networks and Communities, the International ICST Conference on Security and Privacy in Communication Networks, the International Conference on Communication System Software and Middleware, the International Symposium on Modeling and Optimization in Mobile, Ad-Hoc, and Wireless Networks, and the International Conference on Mobile and Ubiquitous Systems: Computing, Networking and Services. He has received numerous professional awards, including a Fulbright Scholarship grant, the ACM Award for Outstanding Contributions to Research on Mobility, and the IEEE Award for Outstanding Technical Contributions to Wireless Personal Communications.